MOSSBAUER EFFECT IN THE ION-IMPLANTED IRON-CARBON ALLOYS

FINAL REPORT

COVERING

JANUARY 1, 1975 THROUGH JUNE 30, 1976

NASA Grant No. NGR-47-020-008

Kwang S. Han

Department of Physical Sciences

Hampton Institute

Hampton, Virginia 23668

TABLE OF CONTENTS

ABSTRACT

The concentration dependence of Mossbauer effect in four carbon ion-implanted iron absorbers, which contain carbon as the solute atoms, has been investigated over the range of concentration 0.05 through 1 atomic percent. The specimens were prepared by implanting carbon atoms on each reference iron foil with four different bombarding energies of 250 kev, 160 kev, 140 kev and 80 kev, respectively. Thus, the specimen contains a uniform dosage of carbon atoms which penetrated up to 3000 A^{o} depth of the reference iron. In the measurement of Mossbauer spectra we used the backscattering conversion electron counting geometry. Typical results of Mossbauer parameters of iron-carbon alloys are as follows:

$d(\text{Isomer shift})/d(\text{carbon concentration}) = +(10.2\pm0.8)\times10^{-3}$ mm/sec/atomic percent,

$d(\text{Quadrupole shift})/d(\text{carbon concentration}) = (4.2\pm0.6)\times10^{-3}$ mm/sec/atomic percent,

$d(g\mu_o H)/d(\text{carbon concentration}) = (4.0\pm0.8)\times10^{-2}$ mm/sec/atomic percent,

$d(g\mu_1 H)/d(\text{carbon concentration}) = (4.35\pm3.03)\times10^{-2}$ mm/sec/atomic percent,

$d(\text{Intensity ratio})/d(\text{carbon concentration}) = -(32.3\pm4.0)\times10^{-13}$ mm/sec/atomic percent,

$d(\Gamma_{1,6})d(\text{carbon concentration}) = (2.0\pm8.0)\times10^{-4}$ mm/sec/atomic percent.

From these data, it is observed that the isomer shift, quadrupole shift, the effective hyperfine splitting of Fe^{57}, and the intensity ratio exhibit the large variation with the increase of carbon concentration in the environment of iron atoms. The isomer shift increases by about 2.5 percent with 1 atomic percent of carbon concentration. The increase of the isomer shift is mainly caused by the increase of 3d electrons at the iron atom sites. About 9 percent increase of quadrupole shift may arise from the electric field gradient at the iron nucleus, in this case, the deviation of the charge

distribution around the nucleus. About 2 percent increase of the effective internal field H at iron atom is mainly attributable to the oscillatory variation in space of the spin polarization of 4s electrons around the iron atom through Fermi contact interaction (Ref. 11). Particularly the contribution of electron spin density at 1st and 2nd nearest neighbor of iron must be large. Since the resolution of satellite absorption lines at 1st and 2nd nearest neighbors from main absorption lines was very poor, it was impossible to determine the effective internal field at 1st and 2nd nearest neighbor of iron, respectively. However, it is found that the effective hfs field measurement could be used to infer the impurity/defect distribution changes needed in Fracture Mechanics Studies.

INTRODUCTION

Mossbauer spectrum is characterized by several parameters whose values are intimately connected with the properties of the nucleus and the electronic charge distribution around it. The electronic environment of the absorber atoms can be modified by chemical process as well as physical process such as the introduction of the impurity into the absorber lattice or the application of the stress (Ref. 3). This modification is reflected in the position and the structure of the resonance lines in the Mossbauer spectrum from which the modified parameters can be determined. It was the purpose of this investigation to determine the effect of the interstitial or substitutional solute atoms on the nuclear energy levels in otherwise pure iron. The nuclear energy levels are sufficiently affected by electronic charge density due to the interstitial or substitutional atoms that information can be gained concerning their states and their interaction with the iron atoms. Furthermore, we can obtain the information about impurity/defect distribution which is of great interest to the solid state physicists as well as the physical metallurgists.

Few interstitial primary solid solutions of iron have been studied, presumably because of their poor solubility (Ref. 1, 2, 4 and 6). For instance, the maximum solubility of the carbon atoms in the alpha iron is only about 0.1 atomic percent at 720°C (Ref. 6).

In the present experiment, up to 1 atomic percent of carbon atoms was introduced into the pure iron, respectively, by the technique of the ion-implantation. With this ion-implantation a high concentration of carbon atoms can be introduced directly into the body centered cubic structure lattice or the interstitial sites (Ref. 17). Consequently, this makes it

possible to obtain appreciable changes in the Mossbauer spectrum of Fe^{57} nuclei, so that a Mossbauer pattern can provide not only the information about the magnetic environment of Fe atoms in ferromagnetic alloy but also a unique way to distinguish between different kinds of iron environment and the migration of the solute atoms into the defective lattice in the solids. The observed Mossbauer spectra at all concentration levels appears to be normal Lorentzian 6-peak patterns observed in the pure iron absorber and are analyzed in order to determine Mossbauer parameters such as isomer shift, Quadrupole shift, hyperfine structure peak position, and linewidth. The results and the interpretation are described below.

EXPERIMENTAL PROCEDURE

Figure 1 shows the general experimental arrangement used for measuring the Mossbauer spectra with the backscattering geometry. A constant acceleration-type spectrometer, in conjunction with a 512 channel pulse height analyzer (Northern Scientific Company, Model 900) permitted measurements over a source-absorber relative velocity up to 16 mm/sec. A 20 millicuries Co^{57} source in a platinum matrix was used as the Mossbauer source. The conversion electron detector counts the 7.3 and 5.6 keV electrons generated by the internal conversion process after the Mossbauer gamma ray is absorbed. This conversion electron detector, through which gas (96% He -4% CH_4) flows at the rate of about 1 cc/min, is operated at 1200 volts. The output pulse of the conversion electron counts were amplified by a preamplifier and a linear amplifier before applying a single channel analyzer. Since the 6.3 keV X-rays emitted by the source constitute the most intense component, a 5 mil thick commercial aluminum absorber was placed in front of the source

to reduce the intensity of 6.3 keV peak by a factor of 10. With the sample absorber in place, 7.3 and 5.6 keV conversion electrons, which were generated by the absorption of 14.4 keV gamma ray, were selected by connecting the output of the single channel analyzer (SCA) to the coincidence input of the multichannel analyzer (MCA). With the coincidence switch of the MCA in "coincidence" position, the upper and lower discriminator levels of a single channel analyzer were adjusted to select the 7.3 and 5.6 keV peak. The SCA output was connected to multi-scale or time mode input of MCA to obtain the Mossbauer spectrum.

Preparation of Sample Absorbers

Iron-Carbon solid solutions were prepared by implanting carbon atoms into the surface of the pure iron foil at KSW Electronics Company. Ion-implantation permits introduction of atoms into the surface layer of a solid substrate by the bombardment of the solids with ions in keV to Mev energy range. In order to make a specimen containing a uniform dosage of carbon atoms which penetrate up to 3000 A°, four different bombarding energies of 250 keV, and 180 keV, 140 keV and 80 keV were used in ion-implantation. The iron specimen for carbon implantation is shown in Table 1. The data about ion-implantation, such as dosage of carbon atoms and the running time are given on the following page.

Furthermore, using L.S.S. theory, the relative distribution of carbon atoms imbedded in the iron foil were calculated against the penetration depth of carbon. Figure 2 shows the relative distribution of carbon atoms in the iron absorber versus the penetration depth.

Bombarding Energy	Dosage	Run Time
Sample #1 (1% Carbon)		
250 kev	$1.54X10^{16}$ ions/cm^2	4440 seconds
160 kev	$1.0X10^{16}$ ions/cm^2	2360 seconds
140 kev	$3.9X10^{15}$ ions/cm^2	1210 seconds
80 kev	$9.0X10^{15}$ ions/cm^2	4320 seconds
Sample #2 (0.5% Carbon)		
250 kev	$7.7X10^{15}$ ions/cm^2	2220 seconds
160 kev	$2.5X10^{15}$ ions/cm^2	1180 seconds
140 kev	$9.0X10^{14}$ ions/cm^2	557 seconds
80 kev	$4.52X10^{15}$ ions/cm^2	2100 seconds
Sample #3 (0.1%)		
250 kev	$1.54X10^{15}$ ions/cm^2	555 seconds
160 kev	$1X10^{15}$ ions/cm^2	393 seconds
140 kev	$3.9X10^{14}$ ions/cm^2	125 seconds
80 kev	$9.0X10^{14}$ ions/cm^2	650 seconds
Sample #4 (0.05% Carbon)		
250 kev	$1.54X10^{14}$ ions/cm^2	60.0 seconds
160 kev	$1.0X10^{14}$ ions/cm^2	40.0 seconds
140 kev	$3.9X10^{13}$ ions/cm^2	20.0 seconds
80 kev	$9X10^{13}$ ions/cm^2	60. seconds

EXPERIMENTAL RESULTS

The Mossbauer spectra were analyzed using a computer program developed at NASA Langley Research Center (Ref. 7). The Analysis provided the values of the following Mossbauer parameter in each spectrum:

I.S.	- Isomer shift of the spectrum.
Q.S.	- Quadrupole Splitting Shift of the spectrum.
$\langle G_0 \rangle$	- Average hyperfine splitting for the ground state in Fe^{57} in the alloy.
$\langle G_1 \rangle$	- Hyperfine splitting for the 14.4 keV state in Fe^{57} in the alloy.
$\langle \Gamma_{1,6} \rangle$	- Average line width for peaks 1 and 6 in the spectrum.
M_2	- Ratio of the sum of the intensities of lines and 1 and 6 to the sum of the intensities of lines 2 and 5 in the spectrum.

The results of Fe-C alloy is summarized in Table 2.

Calibration of the velocity scale for five different iron absorbers was accomplished by using the following reference splitting in a metallic natural iron absorber (Ref. 8).

Splitting between lines 1 and 6 = (10.6248 ± 0.0016) mm/sec
Splitting between lines 2 and 5 = (6.1543 ± 0.0016) mm/sec
Splitting between lines 3 and 4 = (1.6807 ± 0.0016) mm/sec

All measurements were made at room temperature.

Figures 10, 11, 12, and 13 show typical spectrums (backscattered conversion electrons) from the 1/2 mil thick iron absorber containing four different carbon concentrations. It is apparent that there are no evident shoulders to the peaks and the fit between the experimental data and the computed curve based on the least square fitting of the normal Lorentzian 6 peaks is equally good at these different concentrations.

Figures 3 and 4 show the variation of isomeric shift and quadrupole shift as functions of the carbon concentration, respectively. The least squares fit to these data give the following results:

(Isomeric shift in mm/sec) = -(0.4085±0.0016) + (0.0102±0.0008)C Equ. 1

(Quadrupole shift in mm/sec) = (0.0466±0.0006) + (0.0042±0.0006)C Equ. 2

where C is the atomic percent of carbon atoms in the iron absorber. It is seen that the isomeric shift increases by about 2.5% relative to the reference iron absorber as carbon concentration increases to 1 atomic percent, while the change of quadrupole shift is by about 9%. Since the absolute value of quadrupole shift is very small, this variation of quadrupole shift with respect to carbon concentration may be insignificant.

Figures 5 and 6 show $\langle G_o \rangle = g\mu_o H$ and $G = g\mu_1 H$ as functions of carbon concentration, respectively, where g is the nuclear gyromagnetic ration and μ_o and μ_1 the magnetic moment of the ground state and the first excited state of Fe^{57}, respectively, and H the internal magnetic field at the iron nucleus. The least squares fit to these data give the following results:

($\langle G_o \rangle$ in mm/sec) = (4.090±0.037) + (0.040±0.008)C Equ. 3

($\langle G_1 \rangle$ in mm/sec) = (2.231±0.070) + (0.0435±0.0303)C Equ. 4

Since the magnetic moments of the ground state and the first excited state are expected to stay constant, variation of $\langle G_o \rangle$ and $\langle G_1 \rangle$ with respect to carbon concentration implies the corresponding changes in the effective internal magnetic field (H_{eff}) at the iron site (Ref. 3, 9). Equations 3 and 4 show that the effective field H_{eff} increases by about two percent as the carbon concentration increases.

Figures 7 and 8 show the variation of the intensity ration I_1/I_2 and the mean linewidth of the outer peaks (1 and 6) as a function of carbon concentration.

The least squares fit to these data give the following results:

(Intensity ratio I_1/I_2) = (0.719±0.012) - (0.0323±0.004)C Equ. 5

($\langle\Gamma_{1,6}\rangle$ in mm/sec) = (0.264 0.017) + (0.0002±0.0008)C Equ. 6

The examination of Figure 8 shows that the intensity ratio decreases by about 5 percent per atomic percent. This indicates that there exists the strong influence of 1st nearest neighbor (n.n.) and 2nd n.n. carbon atoms. On the other hand, it is apparent that the linewidth is independent of the variation of carbon concentration.

DISCUSSION

As mentioned in the previous section, the isomeric shift of iron spectra for our specimen is negative and is increased by about 2.5 percent. The possible explanation of this tendency will be as follows: The isomeric shift gives a measure of s electron density at the position of the nucleus, $|\Psi(0)|^2$, in case of Fe^{57}, a larger $|\Psi(0)|^2$, gives a more negative isomeric shift. The contribution of 1s and 2s electrons of iron to $|\Psi(0)|^2$ and therefore to isomeric shift cannot be altered, because these electrons also form a complete shell, but their contribution to isomeric shift can be changed by changing the number of 3d electrons in the 3d unfilled. The 3s electrons spend part of their time farther away from the nucleus than 3d electrons, so that an increase in the number of 3d electrons reduces the attractive nuclear potential acting on the 3s electrons and thereby reduces the 3s electron charge density at the nucleus. Therefore, an increase in the number of 3d electron shifts the centroid of the pattern in the positive velocity. This deviation of the isomeric shift from the pure iron also suggests the hybridization of 2s, 2p orbitals of carbon atoms and 3d orbitals of a neighboring iron atom (1st nearest neighbor) forming a covalent bond between them, as Moriya, et al

(Ref. 4)noted. Such an increase in the charge density is expected to be accompanied by the corresponding spin density increase which results in the increased field as observed.

The results on hyperfine splitting indicates that the effective internal field H_{eff} increases by about 2 percent as the population of carbon impurity atom goes up by 1 atomic percent. The slight increase of the internal field at the iron nucleus may be explained as follows: As Genin and Flinn (Ref. 2) noted from their study about the effect of carbon atoms on iron spectra, the presence of carbon atoms may influence the internal field at the iron nucleus in two ways. First, the general expansion of the lattice by carbon atoms at interstitial sites enhance the ferromagnetic interaction in iron and thus the magnetic field at the nucleus for those iron atoms without carbon neighbors. Second, carbon atoms give rise to the oscillatory internal field in space so that the 1st nearest neighbor carbon atom decreases the internal field at the iron nucleus, and the 2nd nearest neighbor carbon atom increases slightly the internal field at the iron nucleus (Ref. 4).

For a more detailed analysis of the spectrum, we calculated the probability of finding carbon atoms at the various interstitial sites with the following equation:

$$P(n,m) = P_n P_m$$

$$= \left[\frac{2 ! C^n (1-C)^{2-n}}{(2-n) ! n !}\right] \left[\frac{4 ! C^m (1-C)^{4-m}}{(4-m) ! m !}\right]$$

Where C = Solute concentration.

For 1 atomic % of carbon concentration, the probability of finding the 1st n.n. Fe's, the 2nd n.n. Fe's, the 3rd n.n. Fe's, etc. are 2.1%, 3.9%, 7.8%, 7.8%, etc., respectively.

If we assume, as a first order approximation, that only the 1st and 2nd n.n. Fe's are strongly affected by carbon atoms, while the remnant iron atoms are entirely in the same state as in the pure iron, then the subtraction of the pure iron spectrum will be 94% that of total absorption intensity of the spectrum. Therefore, if the satellites of the pure iron spectrum were resolved, then the absorption intensity of spectrum due to 1st n.n. and 2nd n.n. Fe's will be 2% and 4%, respectively. Unfortunately, the satellites were not resolved for the following possible reasons:

1. The upper limit of the background counting is about 2% which is almost the same magnitude as the expected absorption intensity of spectrum for 1st nearest neighbor of iron atom.
2. Local micro-environmental fluctuations in a disordered dilute Fe-C alloys smear out the anticipated satellite structure, particularly at the solute concentration levels less than 1 a/o.
3. Statistical fluctuations in the data points smear out any weak structure in the outer peaks in the experimental spectra.

Resolution of the weak satellite lines, if they are observed, could be improved by taking Mossbauer spectra at liquid nitrogen or liquid helium temperature.

It is also noted that the results on the relative intensity ratio of Line 1 and Line 2 considerably deviate from the intensity ratio 3/2 which is based on a 6 line Zeeman splitting of $(3/2^+ \rightarrow 1/2^+)$ line in the absence of any distorting influences. The large deviation of intensity ratio, which is observed in Fe-C alloy, from the value of 3/2 could be explained (Ref. 3, 11). As the population of the solute atom increases, the impurity atoms presumably affect the electron spin alignment in the iron atom, and consequently, polarize the iron nucleus, thereby modifying the relative intensity of $\Delta m = \pm 1$

and $\Delta m=0$ decay with respect to absorber-detector axis. This modified intensity distribution pattern in the $\Delta m=1$ and $\Delta m=0$ resonance peaks should also considerably be reflected in the modified resonance fraction of Fe-C alloy.

Among Mossbauer parameters discussed above, the solute dependence of isomeric shift, effective internal magnetic field and intensity ratio are most marked. Furthermore, the measurement of the hyperfine field at each nearest neighbor of iron nucleus may provide a direct measure of the solute distribution around iron atoms. Such information is of considerable interest in fatigue damage studies and metallic alloys, where impurities are usually in very dilute concentration of solid solution. Periodic hyperfine structure field determination can provide a useful indication of the impurity population build-up in the stress concentration region of the experimental specimen.

CONCLUSION

Mossbauer effect parameters in four ion-implanted iron-carbon alloys have been measured to determine the effect of increasing progressively carbon atoms on host lattice properties. Typical results are summarized:
d(Isomer shift)/d(carbon concentration)=$(10.2\pm0.8)\times10^{-3}$mm/sec/atomic percent,
d(Quadrupole shift)/d(carbon concentration)=$(4.2\pm0.6)\times10^{-3}$mm/sec/atomic percent,
d(g_0H)/d(carbon concentration) = $(4.0\pm0.8)\times10^{-2}$mm/sec/atomic percent,
d(g_1H)/d(carbon concentration) = $(4.35\pm3.03)\times10^{-2}$mm/sec/atomic percent,
d(Intensity ratio)/d(carbon concentration)=$-(32.2\pm4.0)\times10^{-3}$mm/sec/atomic percent,
d($\Gamma_{1,6}$)/d(carbon concentration)=$(2.0\pm8.0)\times10^{-4}$mm/sec/atomic percent.

From the present study of the effect of carbon in the ion-implanted iron alloys, it appears that the isomeric shift, the effective hyperfine field

and intensity ratio exhibit the larger deviation with the increase of the solute concentration. Furthermore, the effective internal field is severely affected by the two first nearest neighbors iron atoms of each carbon atom. These internal fields could be measured by resolving close-lying, low intensity, satellite sextets from the dominant sextet because of large natural width of Fe^{57} hyperfine structure peaks. In order to improve the resolution of weak satellite sextet, we plan to measure the transmission of Mossbauer spectra at the liquid nitrogen temperature and liquid helium temperature. These measurements, hopefully, lead to correlate quantitatively the effective internal field at iron nucleus with the impurity/defect distribution around the stress region, which will be needed in Fracture Mechanics Studies.

REFERENCES

1. P. M. Gielen and R. Kaplow, Acta. Met., 15, 59 (1962)

2. J. M. Genin and P. A. Flinn, Trans. AIME, 242, 1419 (1968)

3. J. J. Singh, NASA. LWP., 865, (1970)

4. T. Moriya, H. Ino, F. E. Fujita and Y. Maeda, J. Phys. Soc. Japan, 24, 60 (1968)

5. H. Ino, T. Moriya, F. E. Fujita, Y. Maeda, S. Ono, and Y. Inokuti, J. Phys. Soc. Japan, 25, 88 (1968)

6. R. P. Elliot, The Constitution of Binary Alloys, First Supplement (McGraw-Hill Book Co., New York, 1965)

7. L. M. Howser, J. J. Singh and R. E. Smith, NASA. Tmx-2522 (1972)

8. J. R. Devoe and J. J. Spikerman, Anal Chem. 42, 366R (1970)

9. J. J. Singh, Bull. Am. Phys. Soc., 18 545 (1973)

10. B. W. Christ and P. M. Giles, Moss. Eff. Meth., 3, 37 (1967)

11. M. B. Stearns, Phys. Rev., 147 439 (1966)

12. H. Cheng and P. A. Bech, ibid 25, 759 (1964)

13. D. O. Van Ostenburg, D. J. Lam, H. D. Trapp, D. W. Pracht, and T. J. Rowland, Phys. Rev. 135 A455 (1964)

14. K. S. Han, Bull. Am. Phys. Soc., 20 92 (1975)

15. K. S. Han, Bull. Am. Phys. Soc., 21 627 (1976)

16. L. C. Feldman, E. N. Kaufmann, J. M. Poate and W. M. Augnstyniak, Ion Implantation in Semiconductor and Other Materials (Plenum Press, New York, 1973) p. 491.

ACKNOWLEDGMENTS

The author wishes to express sincere thanks to the NASA Langley Research Center for financial support and computer support, and to Dr. Jan J. Singh, of NASA Langley Research Center, for his many valuable suggestions.

TABLE 1

COMPOSITION OF THE IRON SPECIMEN FOR CARBON IMPLANTATION

IMPURITY	CONTENT (PPM)	IMPURITY	CONTENT (PPM)
C	10	Mo	-
H	< 1	Na	0.13
O	110	Nb	< 0.1
N	12	Ni	< 1.0
Ag	<0.1	P	1.0
As	0.1	Pd	-
Bi	-	Pt	-
Ca	0.2	Rh	-
Cl	0.8	S	1.0
Co	.07	Si	1.0
Cr	1.0	Sn	-
Cu	0.26	Ta	-
Ga	< 0.1	Ti	< 1.0
Ge	<0.23	V	.03
K	0.13	W	0.1
Mg	1.2	Zn	<0.1
Mn	-	Zr	<0.1

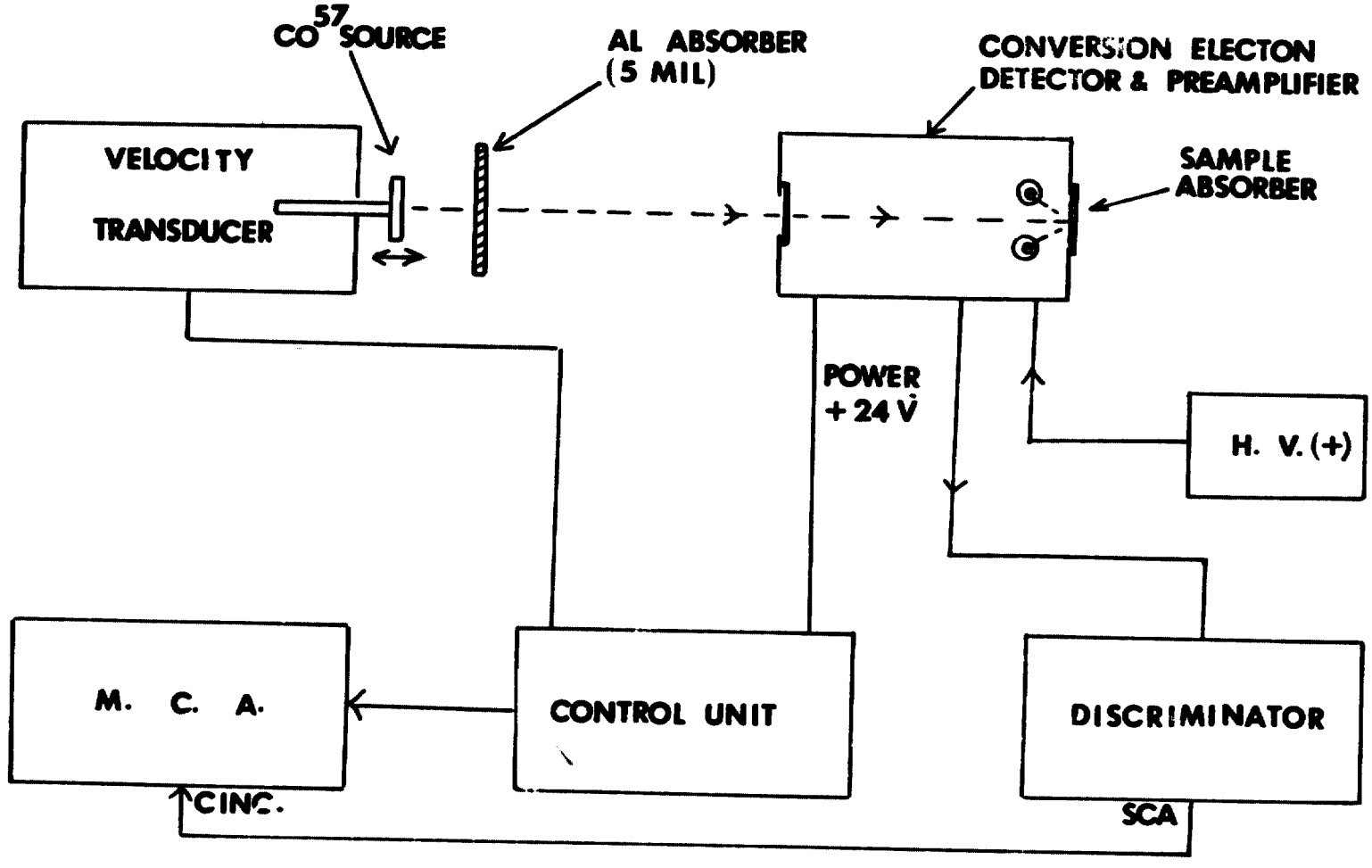

FIG. 1 SCHEMATIC DIAGRAM OF THE EXPERIMENTAL SET UP FOR MEASURING MOSSBAUER SPECTRA WITH A BACKSCATTERING GEOMETRY.

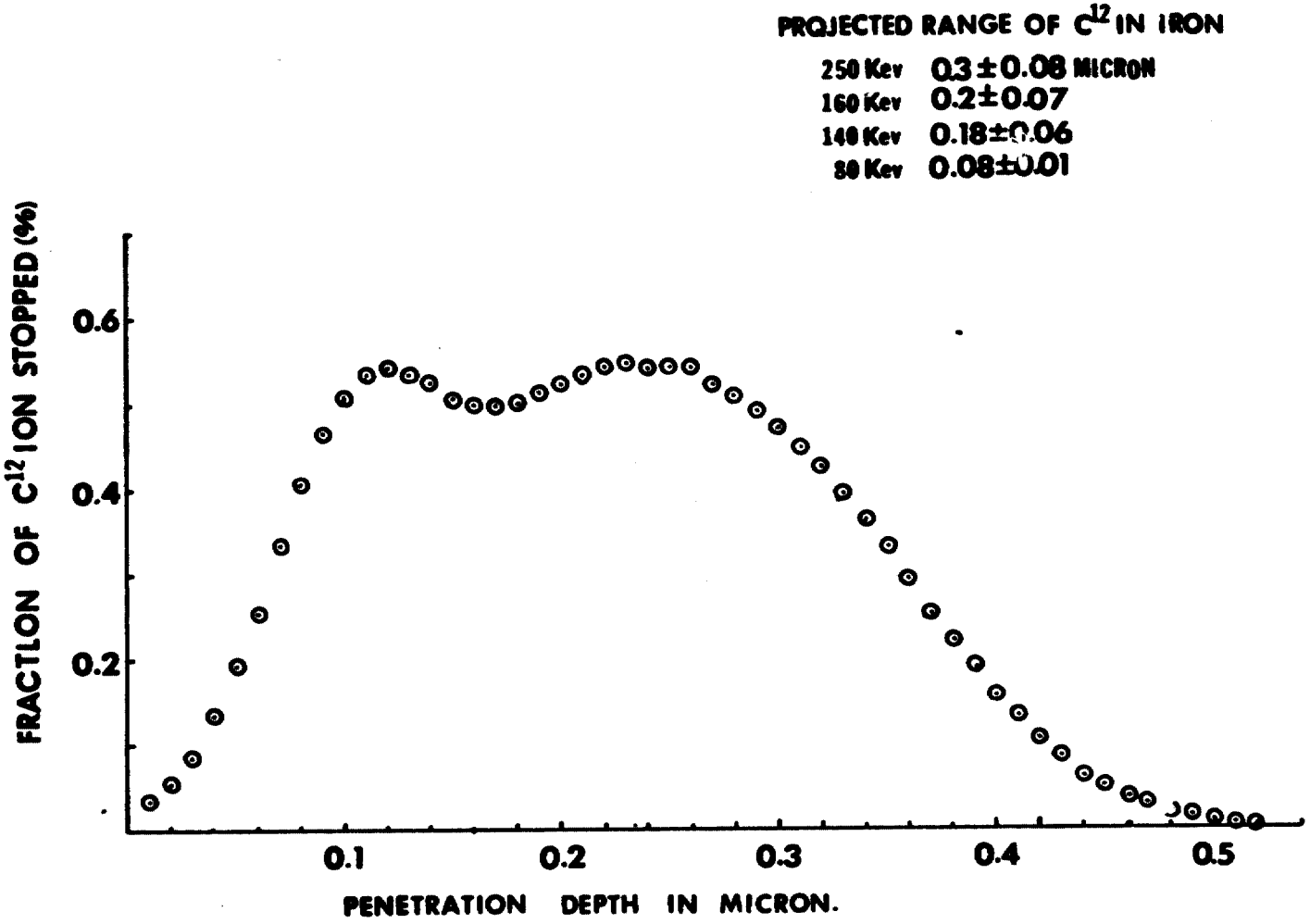

FIG. 2 THE SUPERIMPOSED RANGE DISTRIBUTION OF 80 Kev, 140 Kev, 160 Kev AND 250 Kev C^{12} ION INJECTED INTO Fe TARGET WHERE DOSAGE OF C^{12} IONS ARE 1 ATOMIC PERCENT.

TABLE 2

MOSSBAUER PARAMETERS FOR Fe C ALLOYS FOR VARIABLE C, CONCENTRATION

C CONC. A/O	I.S., MM/SEC	Q.S., MM/SEC	$\langle G_0 \rangle$ MM/SEC	$\langle G_1 \rangle$ MM/SEC	$\langle \Gamma_{1,6} \rangle$ MM/SEC	$M_2 = \frac{A_1 + A_6}{A_2 + A_5}$
0	−0.4102 ± 0.0107	0.0465 ± 0.0107	4.0872 ± 0.0219	2.1976 ± 0.0204	0.2607 ± 0.0260	0.7420 ±
0.05	− 0.4079 ± 0.0067	0.0466 ± 0.0067	4.0927 ± 0.0634	2.2501 ± 0.0258	0.2748 ± 0.0111	0.7171 ±
0.1	−0.4058 ± 0.0120	0.0469 ± 0.0119	4.0920 ± 0.0297	2.2463 ± 0.0249	0.2516 ± 0.0115	0.6904 ±
0.5	−0.4035 ± 0.0062	0.0494 ± 0.0063	4.1182 ± 0.0163	2.2689 ± 0.0140	0.2735 ± 0.0100	0.6998 ±
1.0	−0.3985 ± 0.0086	0.0505 ± 0.0086	4.1258 ± 0.0182	2.2645 ± 0.0201	0.2645 ± 0.0127	0.6900 ±

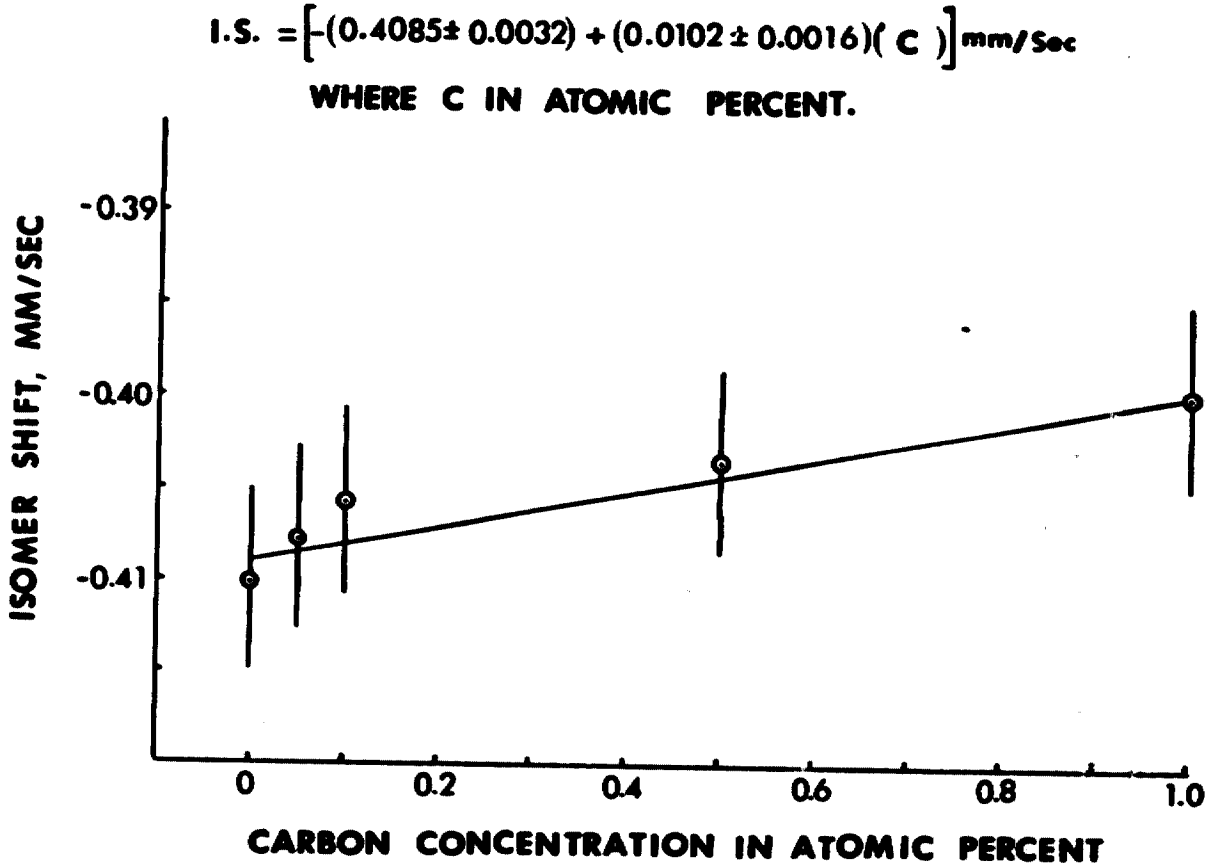

FIG. 3 VARIATION OF ISOMER SHIFT IN CARBON CONCENTRATION.

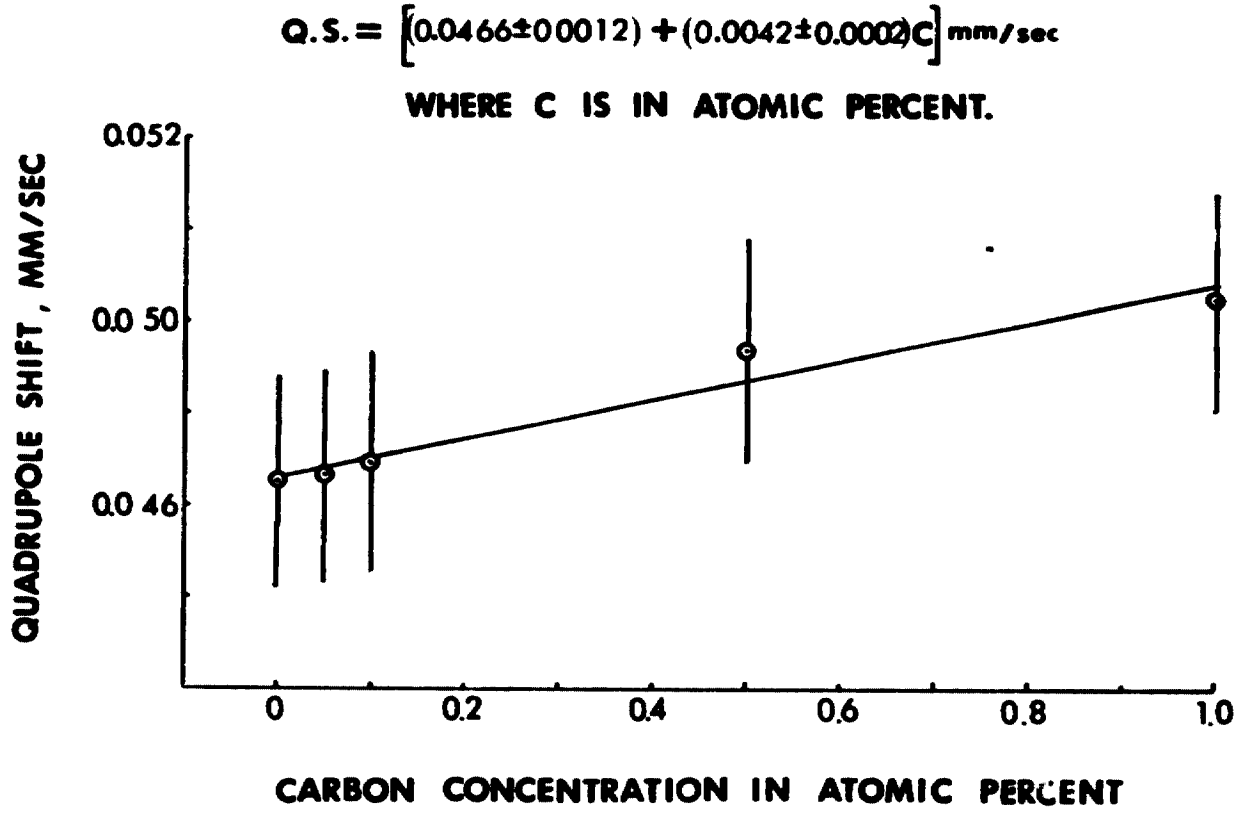

FIG. 4 VARIATION OF QUADRUPOLE INTERACTION IN CARBON CONCENTRATION.

$$\langle G_0 \rangle = \left[(4.090 \pm 00137) + (0.040 \pm 0.008)C\right] \text{ mm/sec}$$

WHERE C IS IN ATOMIC PERCENT.

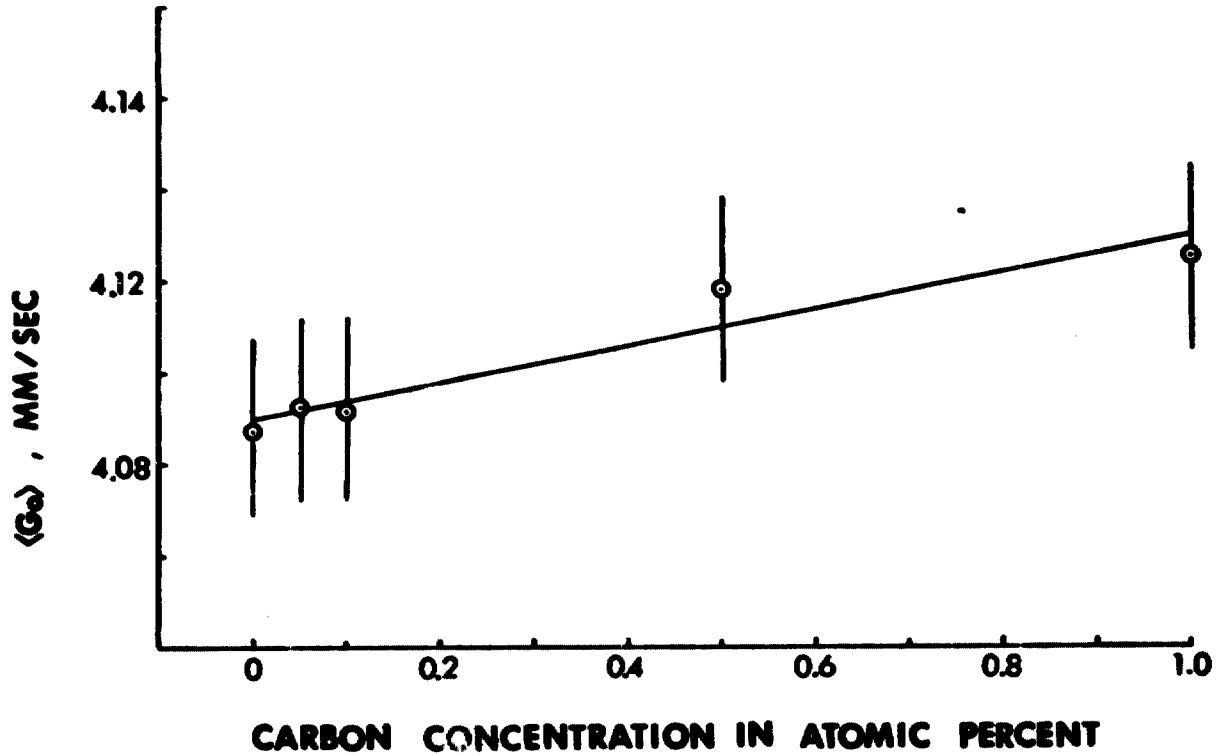

FIG. 5 VARIATION OF GROUND STATE HYPERFINE SPLITTING OF Fe^{57} IN CARBON CONCENTRATION.

$$\langle G_1 \rangle = \left[(2.231 \pm 0.070) + (0.0435 \pm 0.0303)(C) \right] \text{ mm/sec}$$

WHERE C IS IN ATOMIC PERCENT

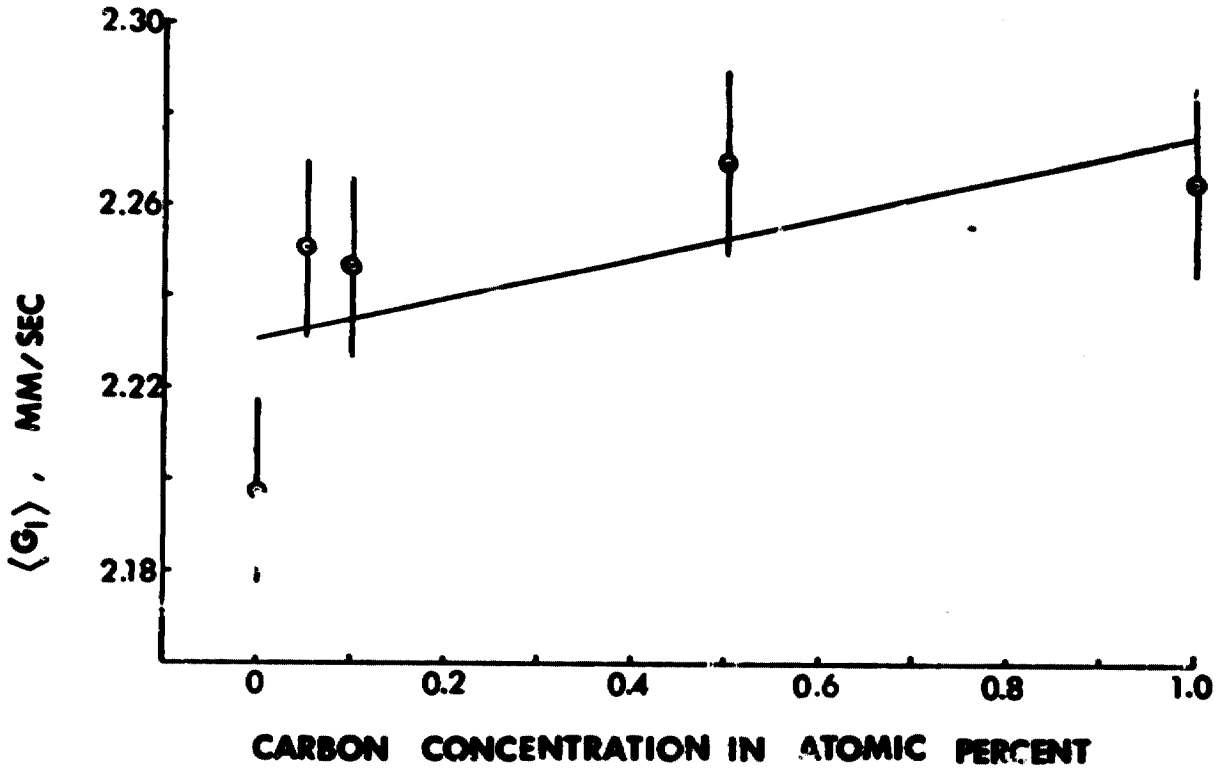

FIG. 6 VARIATION OF FIRST EXCITED STATE HYPERFINE SPLITTING OF Fe^{57} IN CARBON CONCENTRATION.

$$\langle \Gamma_{1,6} \rangle = [(0.264 \pm 0.017) + (0.0002 \pm 0.0008)C]\ \text{mm/sec}$$

WHERE C IS IN ATOMIC PERCENT.

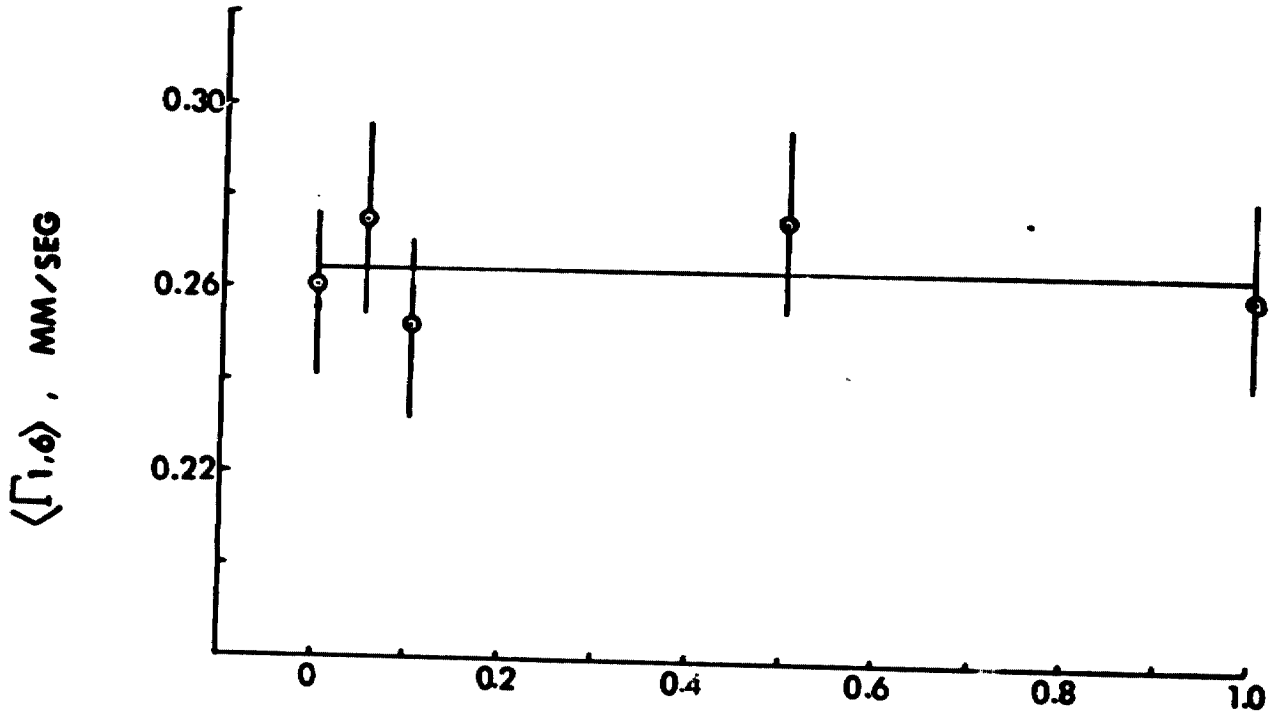

FIG. 7 VARIATION OF OUTER PEAK WIDTHS OF HYPERFINE SPECTRUM OF Fe^{57} IN CARBON CONCENTRATION.

$$M_2 = (0.719 \pm 0.012) - (0.0323 \pm 0.0041)C$$

WHERE C IS IN ATOMIC PERCENT.

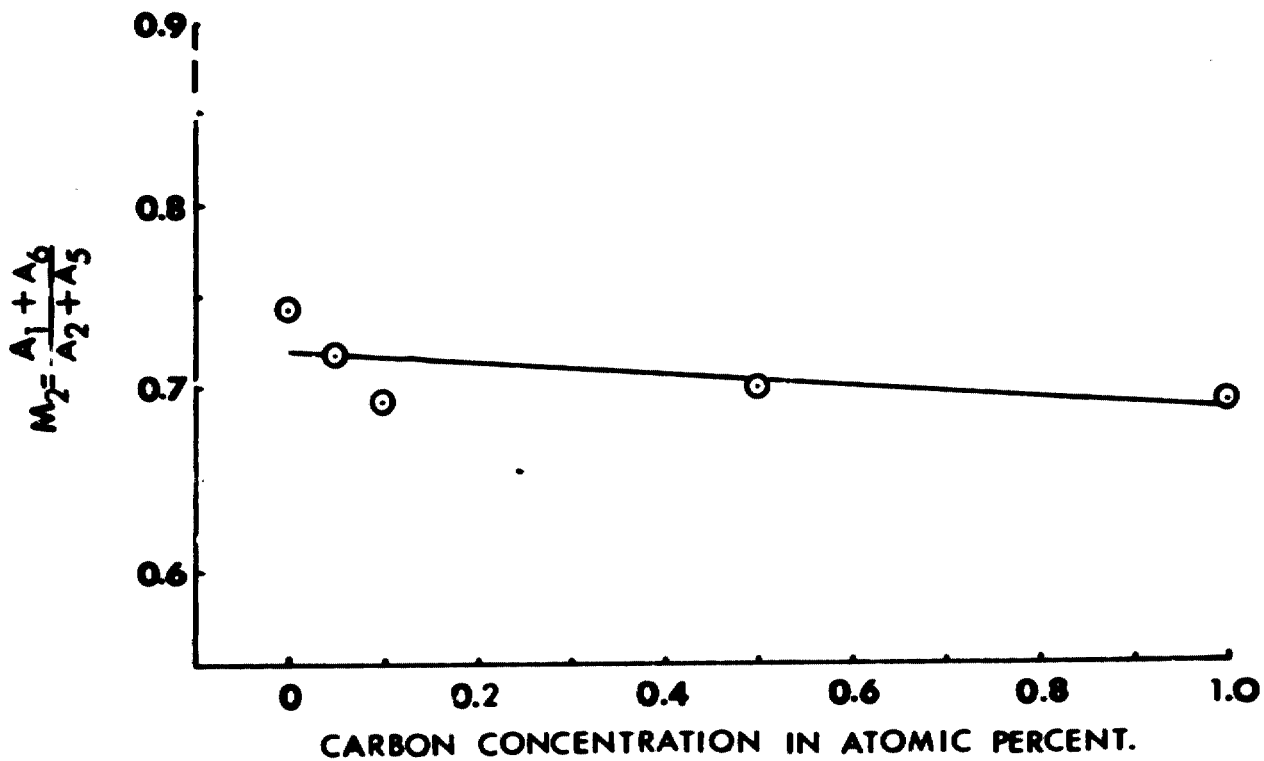

FIG. 8 VARIATION OF M_2 IN Fe-C ALLOY AS A FUNCTION OF C CONCENTION.

FIG.11 A TYPICAL BACKSCATTERED MOSSBAUER SPECTRA IN Fe–C ALLOY

C= 0.1 %

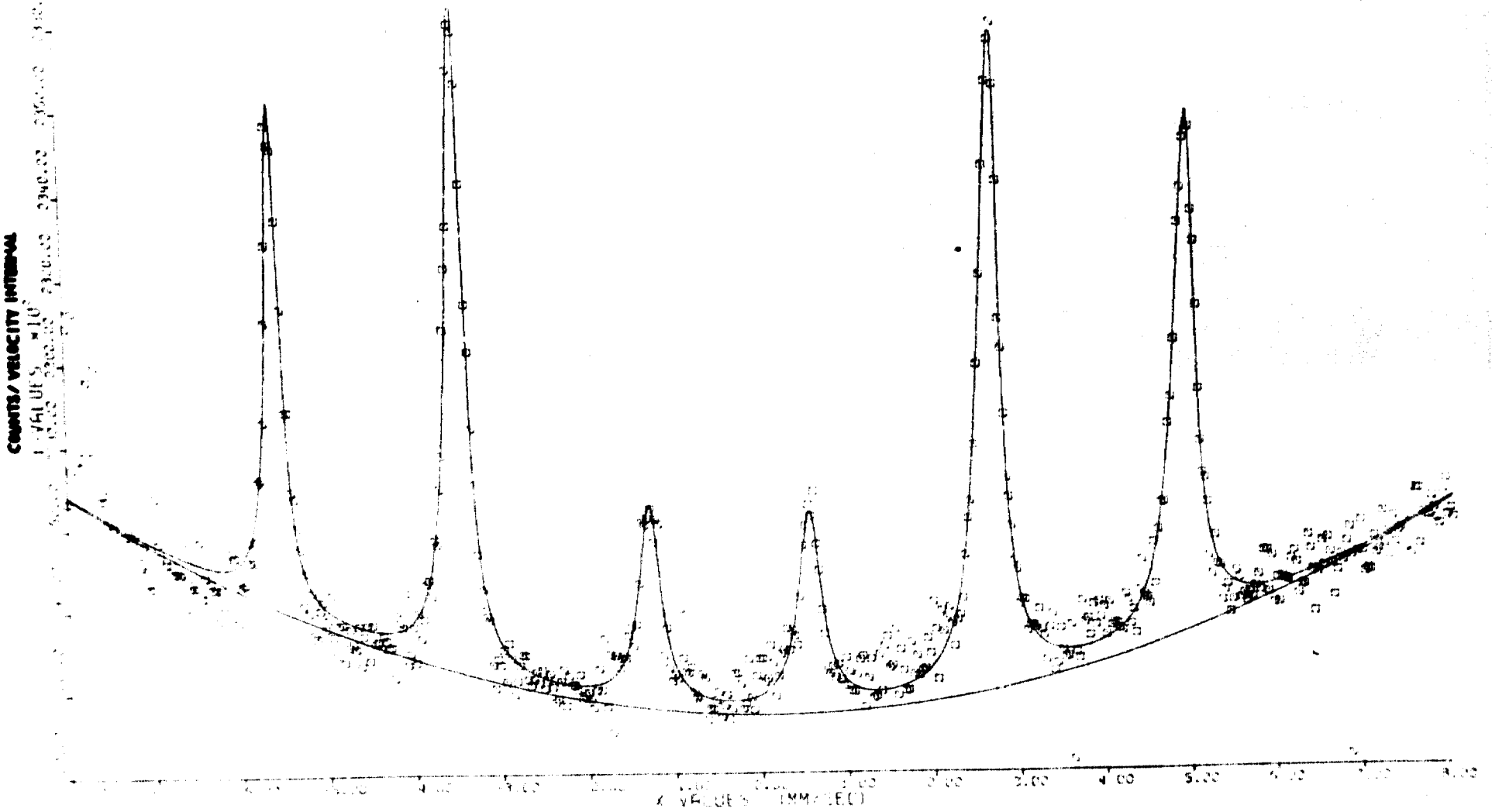

FIG.11 A TYPICAL BACKSCATTERED MOSSBAUER SPECTRA IN Fe–C ALLOY
C= 0.1 %

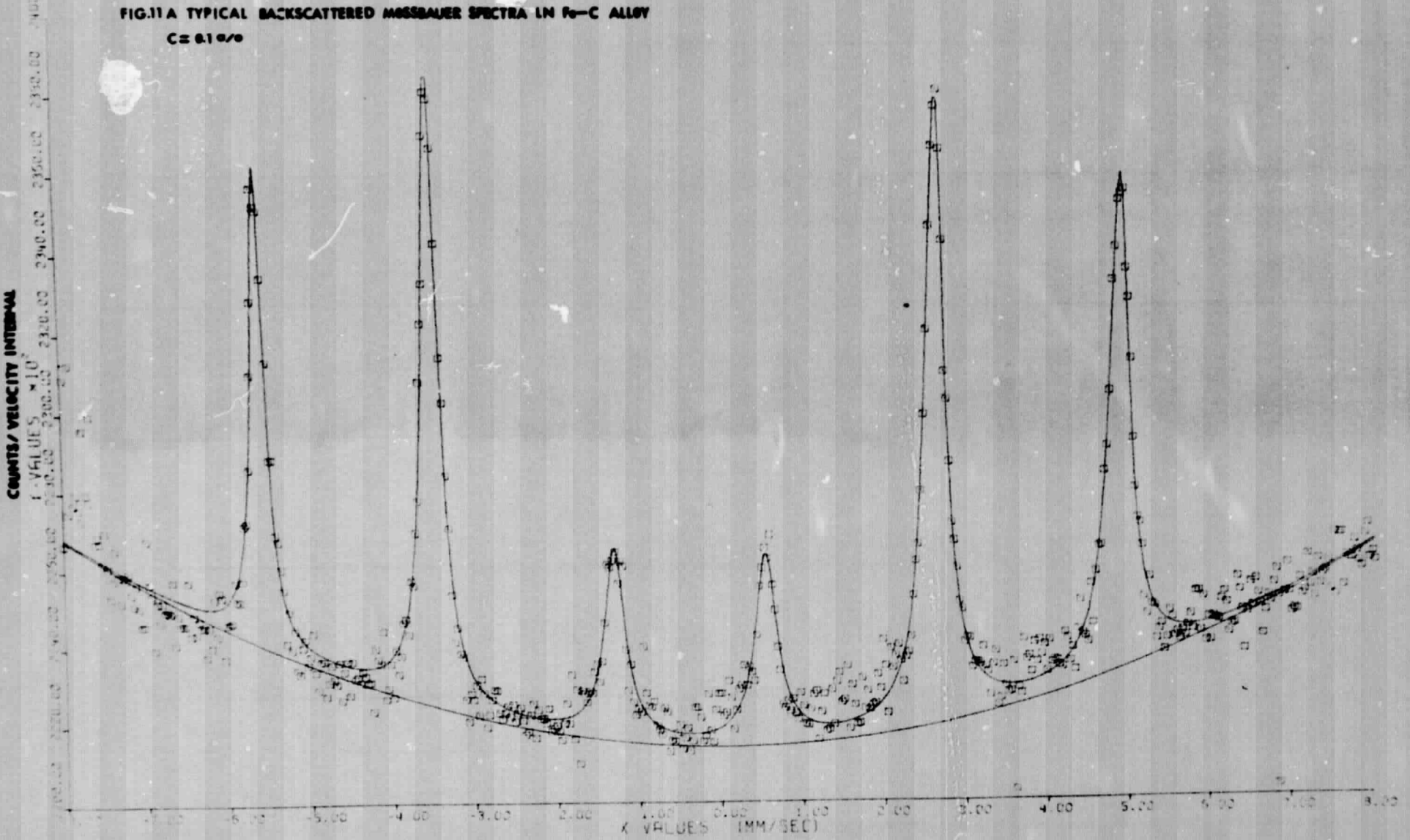

FIG.12 A TYPICAL BACKSCATTERED MOSSBAUER SPECTRA IN Fe–C ALLOY
C = 0.5 %

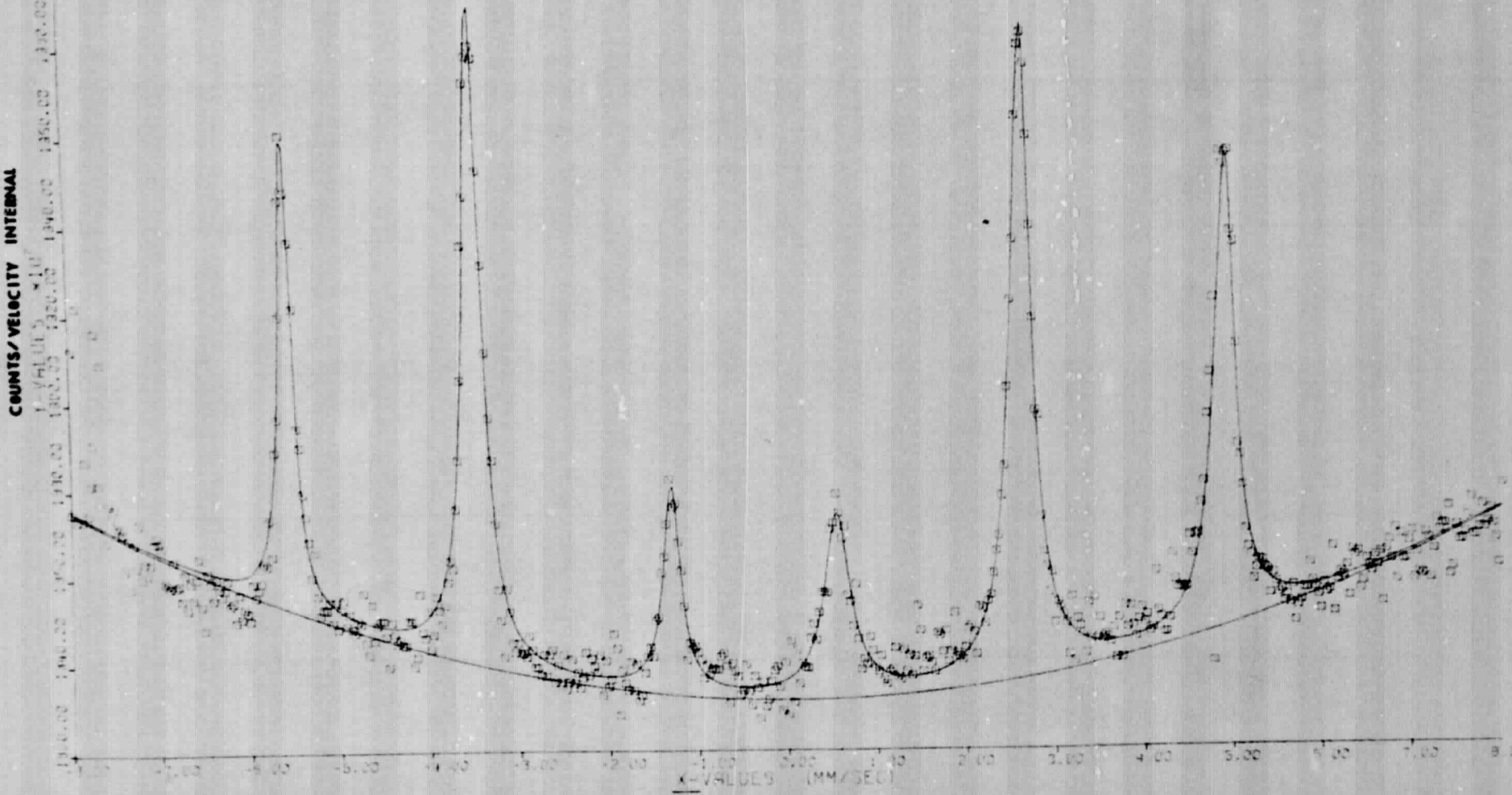

FIG.13 A TYPICAL BACKSCATTERED MOSSBAUER SPECTRA IN Fe—C ALLOY
C = 1%